Topology Optimization of Flywheel Rotors

T. D. Tsai, C. C. Cheng

Advanced Institute of Manufacturing for High-tech Innovations
and Department of Mechanical Engineering
National Chung Cheng University of Taiwan, R.O.C.

imeccc@ccu.edu.tw

Abstract - Flywheels are kinetic energy storage and retrieval devices as chemical batteries. However, the high charge and discharge rates, as well as the high cycling capability make flywheels attractive as compared to other energy storage devices. This research aims for developing a technique based on SIMP method of topology optimization in designing a high-speed rotating flywheel rotor with multi-objective of maximizing the stiffness, the first torsional natural frequency and moment of inertia subject to a limited volume. The design problem is formulated using bound formulation and the method of moving asymptotes (MMA), a first-order optimization technique, was employed. Therefore the design sensitivity becomes a necessity. The so-called checkerboard problem in the topology optimization is avoided using the nodal design variable. Also, a threshold is used to reduce the numerical imperfection in each iteration. The centrifugal force induced in the high-speed rotation is considered in the flywheel topology design. Results show clear topology layout of flywheel was obtained using proposed method. The rib configuration depends both on the rotor acceleration and the centrifugal force induced by the rotational speed.

Keywords – Topology optimization, Flywheel, SIMP

I. INTRODUCTION

Flywheel energy storage (FES) has evolved from simple inertial rotating machines operating at low speeds to fully integrated electro-mechanical batteries. Typical flywheel batteries consist of a high speed inertial rotor, magnetic bearings and the related control system, vacuum housing and containment, power electronics for electrical conversion, etc. Compared with chemical batteries, FES has exceedingly high power and energy density with no fall-off in capacity under repeated charge/discharge cycles; and no degradation during the entire cycle life. All these merits make FES attractive; therefore, it is now considered as enabling technology for many applications. Tensile strength of the material for the rotor is the primary limit to flywheel design. The rotors are optimized for high energy density and limited only by maximum allowable fiber tensile strength.

Designing a flywheel, several issues need to be addressed. The first is to minimize the flywheel torsional vibration. It can be accomplished by increasing the fundamental torsional natural frequency. The second is to maximize the capacity of stored energy. The store energy is proportional to the kinetic energy, so maximizing the stored energy is equivalent in maximizing the moment of inertia of rotor for a given shaft rotational speed. The centrifugal force induced in the high-speed rotation makes the tensile strength of the material for the rotor be the primary limit to flywheel design. Note that the centrifugal force caused by the rotation is design dependent. That is, the force is varying throughout the optimization procedure until the final optimal solution is obtained. The task of maximizing the stiffness and the moment of inertia simultaneously is accomplished using bound formulation.

II. BOUND FORMULATION FOR MAXIMIZING A SPECIFIC EIGENFREQUENCY

The torsional vibration of a flywheel is critical due to three aspects [1]. The first is that the natural frequency corresponding to a torsional mode of a shaft with a flywheel installed on it is lower than the flexural, which implies that the torsional mode of a flywheel system will be easily excited. The second is that the fatigue life for an alternating torsion is shorter than that for an alternating flexure. The third is that the torsional mode itself is a destructive vibration, since it results in failure without showing obvious symptoms. Furthermore, a component is considered to have failed if it vibrates abnormally at critical speeds, even though there is no plastic deformation involved [2]. Therefore, the first objective is to maximize the flywheel fundamental torsional frequency. That is, moving the natural frequencies of flywheel system away from the frequency range of excitation to avoid the resonance is often a basic design requirement.

We start from maximizing the natural frequency of a mechanical system, although this topic has been reported for many years. Ignoring the structural damping, the problem of maximizing a single eigenvalue using bound formulation is formulated as follows [3-5]:

$$\text{Min } -\beta, \tag{1a}$$

subject to:

$$\beta - \lambda_j / \lambda_0 \le 0, \quad j = 1,\ldots,N, \tag{1b}$$

$$(\mathbf{K} - \lambda_j \mathbf{M})\mathbf{\Phi}_j = 0, \quad j = 1,\ldots,N, \tag{1c}$$

$$\mathbf{\Phi}_j^T \mathbf{M} \mathbf{\Phi}_k = \delta_{jk}, \quad j,k = 1,\ldots,N, \tag{1d}$$

$$\sum_{e=1}^{Ne} \rho_e dv - V_0 \le 0, \tag{1e}$$

$$0 < \rho_e \le 1, \quad e = 1, \ldots, Ne, \tag{1f}$$

where λ_j is the jth eigenvalue and the $\mathbf{\Phi}_j$ is the corresponding eigenmode normalized with respect to the kinetic energy, i.e.

$\mathbf{\Phi}_j^T \mathbf{M} \mathbf{\Phi}_j = 1$. $\mathbf{K} = \sum_{e=1}^{Ne} \mathbf{k}_e$ and $\mathbf{M} = \sum_{e=1}^{Ne} \mathbf{m}_e$ are respectively the system stiffness and mass matrices; and $\mathbf{k}_e$, $\mathbf{m}_e$ are the elemental stiffness and mass matrices. V_0 is the volume of the admissible design domain, j, k are the indices of the eigenmode number, and Ne is the number of elements. The density ρ_e is a design variable which correlates the stiffness and the mass matrices as $\mathbf{k}_e = \rho_e^p \mathbf{k}_0$ and $\mathbf{m}_e = \rho_e^q \mathbf{m}_0$ with the power p and q, respectively.

In the optimization, we start from an unpenalized problem (p_0=1) in the first computational cycle and then raises p gradually through the iteration in order to avoid blur topology namely continuation method. The localized mode problem [6-9] usually occurs in free vibration problem due to the unbalanced distribution of material in topology optimization. In this research, the centrifugal forces induced by rotational velocity will cause the similar phenomenon especially at high rotational speed. Threshold values are utilized to overcome this difficulty. An interpolation scheme that an element will be regarded as having zero density when its density is calculated to be below a given threshold value (ρ_{thr}=0.1) is adopted.

Eq. (1) is solved using Svanberg's method of moving asymptotes (MMA) due to its computational efficiency [10]. Nevertheless, it requires the design sensitivity expressed as:

$$\frac{\partial \lambda_j}{\partial x} = \mathbf{\Phi}_j^T \frac{\partial \mathbf{K}}{\partial x} \mathbf{\Phi}_j - \lambda_j \mathbf{\Phi}_j^T \frac{\partial \mathbf{M}}{\partial x} \mathbf{\Phi}_j, \tag{2}$$

Furthermore, the nodal variables instead of density variables are implemented as the design variables to avoid the problems of checkerboard patterns [11-14]. The element volume fraction which traditionally defines the topology is a function of the nodal volume fractions by projecting the nodal value onto the element centroids to determine the element-wise volume fractions.

To avoid a blur topology, a measure of sharpness of the topology layout, called topology quality factor (TQF), is defined by the ratio of the total number of ρ_e>0.9 and ρ_e<0.1 elements to the total number of the remaining elements. The value up to 95% of TQF has been used as one of the stop criterion in the optimization.

III. DESIGN EXAMPLES

Maximizing the fundamental torsional frequency of Flywheel rotor

A design domain of the flywheel is illustrated in Fig. 1. The circle in the middle is a hub of radius 6 cm and the outer circle is a rim with a thickness of 2 cm, and the design domain is the area between the hub and the rim. The material is assumed to be aluminum with a density of 2700 kg/m^3, Poisson ratio of 0.3 and Young's modulus of 70 GPa. The design domain is discretized using 80×80 finite elements, and each element is square with 0.015m of the length of each side. The topology optimization predicts the layout of the structure by determining whether the element inside the design domain is a void or a solid member. Then the residual shape of the structure evolves towards an optimum that satisfies the objective. The material is limited to 50% of the total volume of design domain.

Fig. 2(a) shows the resulting layout before and after the topology optimization using Eq. (1). The fundamental torsional frequency changes from 645 Hz to 797.0 Hz with an increase of 24%.

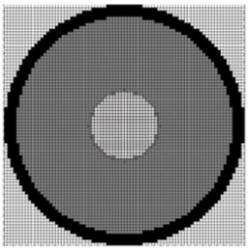

Fig. 1 Design domain of flywheel rotor

A. Maximizing the Moment of Inertia of Flywheel Rotor

As stated in introduction, the second objective is to maximize the moment of inertia for a given shaft rotational speed. For a rotor rotating at a constant speed, maximizing the moment of inertia is formulated as follows:

$$\text{Min } -\beta, \tag{3a}$$

subject to:

$$\beta - I / I_0 \le 0, \tag{3b}$$

Constraints: (1c-f) (3c)

where $I = \sum_{e=1}^{Ne} x_e^q \rho_e v_e r_e^2$ is the moment of inertia, r_e is radius of gyration for element e and I_0 denotes the moment of inertia before optimization. The sensitivity required in the topology optimization is given by

$$\frac{\partial I}{\partial x_e} = q x_e^{q-1} \rho_e v_e r_e^2, \tag{4}$$

Fig. 2(b) shows the resulting layout before and after the topology optimization using Eq. (3). The moment of inertia of flywheel rotor changes from 0.1364 kg-m^2 to 0.1633 kg-m^2 with an increase of 20%. It is not surprising that the rotor mass is concentrated near the rim to achieve the maximal radius of gyration and thus the greatest moment of inertia. However, it is impossible for a flywheel rotor to have a rim but without rib structures that connect with the hub. It reveals that maximizing the moment of inertia cannot be used as the solo objective in the optimization.

It should also be noted that the centrifugal force induced in the high-speed rotation makes the tensile strength of the material for the rotor be the primary limit to flywheel design. That is, the rotors should be optimized for high energy density and limited only by maximum allowable fiber tensile strength. Under this circumstance, the objective for flywheel rotor optimization should include maximizing the rotor stiffness as well as the moment of inertia. That is, the optimization becomes multi-objective or multicriteria, which will be discussed later.

B. Simultaneously Maximizing the Fundamental Torsional Frequency and the Moment of Inertia of Flywheel Rotors

Multicriteria or vector optimization refers to the type of problem in which the objective for optimization is comprised of a set of distinct criteria. The bound

formulation provides a simple method in dealing the structural optimization involved with multipurpose by expressing the min-max problem as a simple minimization problem with bounded objectives. Maximizing the fundamental torsional frequency and the moment of inertia is formulated as follows:

$$\text{Min } -\beta, \tag{5a}$$

subject to:

$$\beta - \lambda_j / \lambda_0 \le 0, \quad j = 1,\ldots,N, \tag{5b}$$

$$\beta - I / I_0 \le 0, \tag{5c}$$

Constraints: (1c-f) (5d)

where Eqs. (5b) and (5c) are the normalized constraints, it is $\lambda_j / \lambda_0 = I / I_0 = 1$ before optimization. With bounded values on the criteria expressed as Eqs. (5b) and (5c), the structural optimization involved with bi-purpose becomes a simple minimization problem. Figure 2(c) shows the resulting topology layout of maximizing the moment of inertia as well as the stiffness of flywheel rotor. It shows the torsional frequency decreases and more mass is distributed near the rim to achieve greater moment of inertia. One may compare it with that from the topology optimization of maximizing the torsional frequency and moment of inertia as shown in Figs. 2(a) and 2(b), respectively. The torsional natural frequency changes from 645 Hz to 761.1 Hz and moment of inertia of flywheel rotor changes from 0.1364 kg-m^2 to 0.1240 kg-m^2.

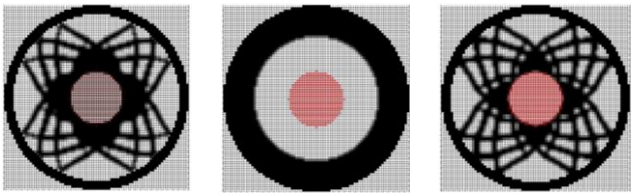

(a) (b) (c)

Fig. 2 Comparison of topology layouts: topology layout of maximizing (a) the fundamental torsional frequency; (b) the moment of inertia and (c) the fundamental torsional frequency and the moment of inertia

C. *Maximizing the Quasi-static Stiffness of Rotating Flywheel Rotors*

As stated previously, for a rotation flywheel, the tensile strength of the material for the rotor is the primary limit to flywheel design. The rotors should be optimized for high energy density as well as maximal tensile strength. Maximizing the stiffness or minimizing the compliance of structures has been studied for many years. However, maximizing the stiffness of a rotating structure is seldom reported. Consider the design domain as shown in Fig. 3 where a hub of radius 6 cm is located at the center with all degrees of freedom fixed within its circumference and the outer circle is a rim with a thickness of 2 cm similar as in Fig. 1. The inertia force induced by angular acceleration is simplified as eight loads $\mathbf{F}_t$ with 100 Nt each applied evenly on the rim at counterclockwise direction. The design domain is meshed using 80 by 80 four-node finite elements. Each element is square with 0.015m of the length of each side. Maximizing the rotating flywheel rotor stiffness is formulated as follows:

$$\text{Min } -\beta, \tag{6a}$$

subject to:

$$\beta - \frac{\mathbf{F}_{tc0}^T \mathbf{U}_{tc0}}{\mathbf{F}_{tc}^T \mathbf{U}_{tc}} \le 0, \tag{6b}$$

$$\mathbf{K}\mathbf{U}_{tc} = \mathbf{F}_{tc} = \mathbf{F}_t + \mathbf{F}_c, \tag{6c}$$

$$\sum_{e=1}^{Ne} \rho_e dv - V_0 \le 0, \tag{6d}$$

$$0 < \rho_e \le 1, \quad e = 1, \ldots, Ne, \tag{6e}$$

where $\mathbf{F}_{tc}$=$\mathbf{F}_t$+$\mathbf{F}_c$ is the external force including the centrifugal force $\mathbf{F}_c$ induced by rotation and the inertia force $\mathbf{F}_t$ caused by accelerating or decelerating the rotor. $\mathbf{U}_{tc}$ represents the displacement caused by $\mathbf{F}_t$ and $\mathbf{F}_c$. Note that the objective is normalized with respect to the compliance before the optimization, i.e. $\mathbf{F}_{tc0}^T \mathbf{U}_{tc0}$ for quasi-static compliance. In most cases of flywheel, the rotor is installed inside a vacuum container. If the rotor rotates at a constant speed, $\mathbf{F}_t$ is zero. However, $\mathbf{F}_t$ is not zero when the flywheel is accelerating or decelerating. As for the centrifugal force that is proportional to the rotating speed is expressed as:

$$\mathbf{F}_c = \sum_{e=1}^{Ne} x_e^q \rho v_e \omega^2 r_e, \tag{6f}$$

where ω is the rotational speed, r_e is radius of gyration for element e. The sensitivity is expressed as:

$$\frac{\partial\left(\mathbf{F}_{tc}^T \mathbf{U}_{tc}\right)}{\partial x} = -\mathbf{U}_{tc}^T \frac{\partial \mathbf{K}}{\partial x} \mathbf{U}_{tc} + 2\mathbf{U}_{tc}^T \frac{\partial \mathbf{F}_c}{\partial x}, \tag{7}$$

where

$$\frac{\partial \mathbf{F}_c}{\partial x} = q x_e^{q-1} \rho v_e \omega^2 r_e, \tag{8}$$

Figure 4 shows the topology layout of the flywheel rotor in varying rotational speed ranging at 0, 1000 and 5000 RPM. When the rotor is static, i.e. 0 RPM, the resulting layout is the same as that without centrifugal force. With the rotational speed increasing, the rib of flywheels becomes curved and the rib tip bends towards to the opposite direction to that of flywheel rotation. As the rotational speed increases to a very high value, the rib appears straight. The degree in bending of ribs depends on the ratio of centrifugal forces and the inertia force caused by acceleration. TABLE I compares the static compliance, quasi-static compliance, moment of inertia and first natural frequency of the topology layout after optimization.

Note that when the rotational speed increases, the centrifugal force increases greatly and becomes much larger than the inertia force caused by acceleration. As a result, the optimal layout as shown in Figure 4(c) becomes very weak in the circumferential direction with a compliance of 8.75×10^{-5}J. It concludes that minimizing the dynamic compliance must be accompanied with a constraint in static compliance at the same time [15]. Thus, a multi-criteria formulation for simultaneously increasing the static and quasi-static stiffness is introduced in the next section.

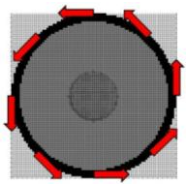

Fig. 3 Design domain and the inertia forces of a rotating flywheel rotor

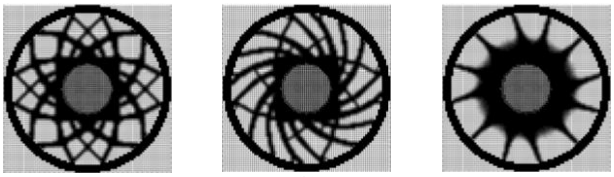

(a) (b) (c)

Figure 4 The topology layout of the flywheel rotor with an objective of maximizing the rotor stiffness; (a) 0 RPM; (b) 1000 RPM; (c) 5000 RPM

TABLE I
MAXIMIZING THE ROTOR QUASI-STATIC STIFFNESS

RPM	Static compliance (J)	Quasi-static compliance (J)	Moment of inertia (kg-m^2)	First frequency (Hz)
0	3.70×10^{-5}	3.70×10^{-5}	0.1203	784.3
1000	4.55×10^{-5}	3.95×10^{-5}	0.1199	709.0
5000	8.75×10^{-5}	0.0039	0.1090	575.5

D. Simultaneously Maximizing the Static and Quasi-static Stiffness of the Rotating Flywheel Rotor

To prevent the weak stiffness optimal layout at high rotational speed as illustrated in Fig. 4(c), simultaneously maximizing both static and quasi-static stiffness of the rotating flywheel rotor is formulated as follows:

$$\text{Min } -\beta, \tag{9a}$$

subject to

$$\beta - \frac{\mathbf{F}_{t0}^T \mathbf{U}_{t0}}{\mathbf{F}_t^T \mathbf{U}_t} \le 0, \tag{9b}$$

$$\mathbf{K}\mathbf{U}_t = \mathbf{F}_t, \tag{9c}$$

Constraints: (6b-e) (9d)

The difference between the static and quasi-static compliances is that the latter considers the centrifugal forces induced by the rotation. $\mathbf{U}_{tc}$ represents the displacement caused by both $\mathbf{F}_t$ and $\mathbf{F}_c$, and $\mathbf{U}_t$ represents the displacement caused by $\mathbf{F}_t$ only. Note that the objective is normalized with respect to the compliance before the optimization, i.e. $\mathbf{F}_{tc0}^T \mathbf{U}_{tc0}$ for quasi-static compliance and $\mathbf{F}_{t0}^T \mathbf{U}_{t0}$ for static compliance respectively.

Figure 5 shows the topology layout of the flywheel rotor in varying rotational speed ranging at 0, 1000 and 5000 RPM. When the rotor is static, i.e. 0 RPM, the resulting layout is the same as that without centrifugal force. With the rotational speed increasing, fewer ribs appear due to the increase of the centrifugal forces.

Compare the TABLE I and TABLE II, they have little difference in quasi-static compliance. However, minimizing the quasi-static compliance results in low static stiffness at high rotational speed, and this shortcoming can be overcome by simultaneously minimizing the quasi-static and static compliance.

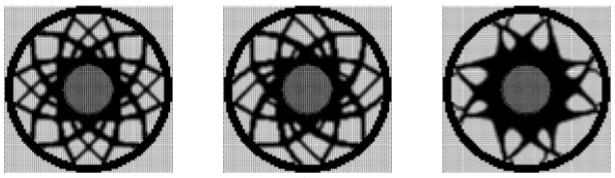

(a) (b) (c)

Figure 5 The topology layout of the flywheel rotor with an objective of maximizing the rotor stiffness; (a) 0 RPM; (b) 1000 RPM; (c) 5000 RPM

TABLE II
THE RESULTS OF SIMULTANEOUSLY MAXIMIZING THE ROTOR QUASI-STATIC AND STATIC STIFFNESS

RPM	Static compliance (J)	Quasi-static compliance (J)	Moment of inertia (kg-m^2)	First frequency (Hz)
0	3.70×10^{-5}	3.70×10^{-5}	0.1203	784.1
1000	3.78×10^{-5}	4.27×10^{-5}	0.1193	776.6
5000	4.55×10^{-5}	0.0048	0.1126	759.1

E. Simultaneously Maximizing the Rotating Flywheel Rotor Quasi-Static and Static Stiffness and Moment of Inertia

Maximizing the quasi-static, the static stiffness and the moment of inertia of the rotating flywheel rotor simultaneously is formulated as follows:

$$\text{Min } -\beta, \tag{10a}$$

subject to

$$\beta - \frac{I_r}{I_{r0}} \le 0, \tag{10b}$$

Constraints: (6b-e), (9b, 9c) (10c)

where Eqs. (6b), (9b) and (10b) are bounded criteria including the quasi–static compliance, the static compliance and the moment of inertia, respectively. Figure 6 shows the topology layout of maximizing the three normalized objective simultaneously. From TABLE III, it is not surprising that the resulting topology layout has a better moment of inertia but less static compliance as compared to those in TABLE II.

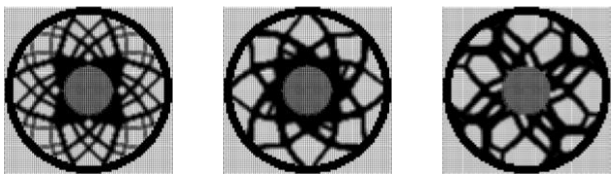

(a) (b) (c)

Figure 6 The topology layout of the flywheel rotor with an objective of maximizing the rotor stiffness and kinetic energy; (a) 0 RPM; (b) 1000 RPM; (c) 5000 RPM

TABLE III
THE RESULTS OF SIMULTANEOUSLY MAXIMIZING THE ROTOR QUASI-STATIC AND STATIC STIFFNESS AND THE MOMENT OF INERTIA

RPM	Static compliance (J)	Quasi-static compliance (J)	Moment of inertia (kg-m^2)	First frequency (Hz)
0	3.88×10^{-5}	3.88×10^{-5}	0.1208	759.9
1000	3.84×10^{-5}	4.52×10^{-5}	0.1196	761.2
5000	4.99×10^{-5}	0.0050	0.1275	639.4

IV. CONCLUSIONS

Conceptual design of flywheel rotor using topology optimization is presented. A high-speed rotating flywheel rotor with respective to objective such as maximal fundamental torsional natural frequency, maximal moment of inertia, maximal stiffness and theirs combination as well are studied subject to a limited volume. The centrifugal force induced in the high-speed rotation is considered in maximizing the stiffness of flywheel topology design. The method of moving asymptotes (MMA), a first-order optimization technique, was employed, which requires the design sensitivity. The so-called checkerboard problem in the topology optimization is avoided utilizing the nodal design variable. Results show the clear topology layout of flywheel was obtained using proposed method. The rib of flywheels becomes curved and the rib tip bends towards to the opposite of flywheel rotational direction when the rotational speed increases. The rib configuration depends on the rotor acceleration and the centrifugal force induced by the rotational speed. Moreover, simultaneously minimizing both the quasi-static and the static compliances have an apparent advantage in static stiffness compare to minimizing the quasi-static compliance alone.

ACKNOWLEDGMENT

This work was partially supported by the National Science Council of Taiwan, Republic of China under Contract No. NSC 98-2622-E-194-004-CC2. The support of the MMA Matlab code from Krister Svanberg is much appreciated.

REFERENCES

[1] V. Prakash, M. R. Vadiraj, D. N. Venkatesh, and U. Shrinivasa, "Parametric study of crankshaft natural frequencies," SAE paper, 940698, (1994).

[2] P. J. Carrato, and C. C. Fu, "Modal analysis for torsional vibration of diesel crankshafts," SAE paper, 861225, (1986).

[3] J. Du, N. Olhoff, "Topological design of freely vibrating continuum structures for maximum values of simple and multiple eigenfrequencies and frequency gaps," *Structural and Multidisciplinary Optimization*, 34 (2007) 91–110.

[4] J. Du, N. Olhoff, "Topology optimization of continuum structures with respect to simple and multiple eigenfrequencies," Proceedings of the 6th World Congresses of Structural and Multidisciplinary Optimization, Rio de Janeiro, Brazil, (2005)

[5] J. S. Jensen, N. L. Pedersen, "On maximal eigenfrequency separation in two-material structures: the 1D and 2D scalar cases," *Journal of Sound and Vibration*, 289 (2006) 967-986.

[6] N. L. Pedersen, "Maximization of eigenvalues using topology optimization," *Structural and Multidisciplinary Optimization*, 20 (2000) 2-11.

[7] N. L. Pedersen, "Topology optimization of laminated plates with prestress," *Computers and Structures*, 80 (2002) 559-570.

[8] D. Tcherniak, "Topology optimization of resonating structures using SIMP method," *International Journal for Numerical Methods in Engineering*, 54 (2002) 1605–1622.

[9] J. Du, N. Olhoff, "Topological design of freely vibrating continuum structures for maximum values of simple and multiple eigenfrequencies and frequency gaps," *Structural and Multidisciplinary Optimization*, 34 (2007) 91–110.

[10] K. Svanberg, "The method of moving asymptotes-a new method for structural optimization," *International Journal for Numerical Methods in Engineering*, 24 (1987) 359–373.

[11] C. S. Jog, R. B. Haber, "Stability of finite element models for distributed-parameter optimization and topology design," *Computer Methods in Applied Mechanics and Engineering*, 130 (1996) 203-226.

[12] K. Matsui, K. Terada, "Continuous approximation of material distribution for topology optimization," *International Journal for Numerical Methods in Engineering*, 59 (2004) 1925-1944.

[13] S. Rahmatalla, C. C. Swan, "Form finding of sparse structures with continuum topology optimization," *Journal of Structural Engineering*, 129 (2003) 1707-1716.

[14] S. F. Rahmatalla, C. C. Swan, "A Q4/Q4 continuum structural topology optimization implementation," *Structural and Multidisciplinary Optimization*, 27 (2004) 130-135.

[15] N. Olhoff, J Du, "Topological design of continuum structures subjected to forced vibration," Proceedings of the 6th World Congresses of Structural and Multidisciplinary Optimization, Rio de Janeiro, Brazil (2005)